

Department of Physics and Measurement Technology

Configuration of a pulse radiolysis system for the study of gas-phase reactions and kinetic investigations of the reactions of hydroxyl radicals with methyl and ethyl radicals.

Linköping Studies in Science and Technology, Chemical Physics

Thesis No. 357

Kjell Fagerström

LiU-TEK-LIC-1992:49

ISSN 0280-7971

ISBN 91-7871-051-0

Linköping January 1993



**Configuration of a pulse radiolysis system for the study
of gas-phase reactions and kinetic investigations of the
reactions of hydroxyl radicals with methyl and ethyl
radicals.**

Linköping Studies in Science and Technology, Chemical
Physics

Thesis No. 357

Kjell Fagerström

LiU-TEK-LIC-1992:49

ISSN 0280-7971

ISBN 91-7871-051-0

Linköping January 1993

Table of contents

| | |
|---|----|
| PREFACE | 2 |
| 1 INTRODUCTION | 3 |
| 2 PULSE RADIOLYSIS | 3 |
| 3 REACTION KINETICS | 4 |
| 4 EXPERIMENTAL SECTION | 6 |
| 4.1 Non-Beer's law behaviour | 6 |
| 4.2 Wall reactions | 10 |
| 4.3 The maximum radical concentration in different bath gases | 11 |
| 4.4 Kinetics of the reaction between methyl and hydroxyl radicals | 13 |
| ACKNOWLEDGEMENTS | 17 |
| REFERENCES | 18 |
| SUMMARY OF PAPERS | 19 |
| PAPERS 1 - 3 | |

Preface

The work presented in this thesis was performed during the period January 1990 to December 1992. During the first 18 months of this period the work was focused on the configuration of a pulse radiolysis system for kinetic studies of gas-phase reactions. Experimental investigations of the kinetics of some reactions involved in hydrocarbon combustion processes have been performed during the last 18 months.

This thesis is divided into two parts, the first of which gives an introduction to the subject as well as a description of experiments and calculations not included in any of the three original papers that are included in the second part. The papers presented in the second part are:

- 1 **A computerised pulse radiolysis system for gas phase kinetics**
K. Fagerström, A. Lund, P. Pagsberg and A. Sillesen
Submitted for publication to Acta Chem. Scand.

- 2 **Kinetics of the cross-reaction between methyl and hydroxyl radicals**
K. Fagerström, A. Lund, G. Mahmoud, J. Jodkowski and E. Ratajczak.
Accepted for publication in Chemical Physics Letters.

- 3 **Kinetics of the gas-phase reaction between ethyl and hydroxyl radicals**
K. Fagerström, A. Lund, G. Mahmoud, J. Jodkowski and E. Ratajczak.
Submitted for publication to Chemical Physics Letters.

1 Introduction

The importance of reactions involved in hydrocarbon combustion processes cannot be overemphasized. A vast chemical industry exists based on the feedstocks produced by the controlled pyrolysis of hydrocarbons, while uncontrolled combustion in air is still among the most important sources of heat and mechanical energy. Most of the energy consumed in the world is produced in hydrocarbon combustion processes.

It is very difficult to predict in detail the behaviour of any combustion system involving hydrocarbons. One reason is that too few reactions have been studied under conditions anywhere near those existing during combustion. More interest has been shown in the chemistry of polluted atmospheres than in the chemistry of the source of those pollutants.

The reaction scheme for any hydrocarbon consists of many steps, with branching dependent on the physical conditions, and involves tens and even hundreds of various compounds. It is therefore difficult to give a general mechanism for the complete hydrocarbon oxidation reaction.

The work that is presented in this thesis deals with the assembling and testing of a pulse radiolysis system for kinetic studies of gas-phase reactions as well as with the kinetics of the gas-phase reactions of hydroxyl radicals with methyl and ethyl radicals. These radicals are very important as these are formed at an early stage in hydrocarbon combustion processes. The two studied reactions are key reactions in those processes.

2 Pulse radiolysis

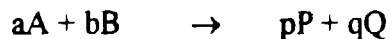
The technique that was used to generate the studied free radicals is pulse radiolysis, which is the radiation-chemical equivalent of flash photolysis in which the initiating flash illumination is replaced by an electron pulse. This

means that the free radicals are generated by electron irradiation of stable parent gas mixtures. Flash photolysis is more frequently used than pulse radiolysis. The number of systems that can be studied with pulse radiolysis is wider than with flash photolysis because these are not restricted to those that can be excited photochemically. Pulse radiolysis is a very clean source of radicals and a rather high radical concentration can be obtained. This means that the method is very useful for studies of radical-radical reactions. Typically, these reactions occur on a time scale from a few micro to a few milli seconds. The energy dissipated as heat is considerably low in pulse radiolysis which simplifies the temperature control of the reaction vessel. A limitation of the method is that several radicals may be produced by the electron pulse. This unwanted situation can often be circumvented by clever utilization of radical chemical reactions to enhance the formation of a specific radical.

In this case the electrons were generated by a Febetron 708, which is an electron accelerator of the field emission type and UV absorption spectrometry was used to detect the generated free radicals. Light from a high-intensity xenon lamp was passed through the reaction cell containing the sample to be irradiated and further to a monochromator and a photomultiplier. The signal from the photomultiplier was fed to an oscilloscope and an electronic digitizer. In use, the monochromator is set to a wavelength at which one of the expected transient species or products absorbs.

3 Reaction kinetics

The rate of reaction is defined as the rate of change of concentration for reactants or products [1]. In the following reaction:



the rate, R, may be expressed as:

$$R = -d[A]/dt = -(a/b)(d[B]/dt) = (a/p)(d[P]/dt) = (a/q)(d[Q]/dt)$$

where the terms in square brackets are the concentrations and a, b, p and q denote the number of moles of each species. The negative signs indicate that during reaction the reactant concentration decreases.

The rate of a chemical reaction depends of several factors in addition to reactant concentration. In some cases the rate is influenced by the products, substances such as catalysts, or even chemically inert species. The rate is also temperature dependent.

The variation of the experimentally measured rate with reactant concentration may often be expressed by the following equation:

$$R = k[A]^x[B]^y \dots$$

This is the experimental rate equation and it shows that the rate is usually proportional to each reactant concentration raised to some power. These experimentally determined exponents (x, y...) are called the partial orders of reaction. The sum of the partial orders is the overall order of reaction. The orders of reaction are often integers, but are not necessarily so. For the great majority of reactions these numbers are between 0 and 3. Experimental measurements of reaction order can provide important insight into the molecular detail of a reaction. The proportionality constant, k, in the rate equation, is the reaction rate constant. The rate constant varies with temperature.

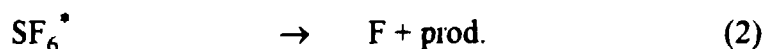
4 Experimental section

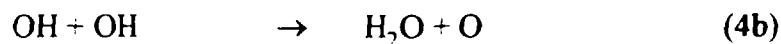
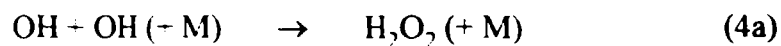
In this section experiments and calculations not, or just partly, included in the three original papers are described. All the experiments were performed at room temperature.

Note: The maximum concentration of radicals generated in the described experiments can vary from experiment to experiment. One reason for this is that the electron accelerator was taken apart twice for renovation during this experimental period and the electron dose was not exactly the same after the renovations as before. During one of those renovations the thin electron windows in the reaction cell (see Figure 2 in Paper 1) were replaced. The new ones are somewhat thicker than the old ones. This reduced the electron dose. Another reason is that sometimes the charging voltage had to be kept below the normal 30 kV due to self triggering.

4.1 Non-Beer's law behaviour

In gas-phase studies, absorption spectra of transient species often consist of discrete lines or very sharp peaks. This is the case with the hydroxyl radical which has a strong, very sharp absorption peak at 309 nm. The minimum band pass of the monochromator is much wider than the width of the OH peak. In such a case the Beer-Lambert law is not obeyed; that is the relation $A = \epsilon cL$ (where ϵ is the extinction coefficient and L is the optical path length) is not correct. The absorbance, A , can be calculated either as $A = \log(I_0/I)$ or as $A = \ln(I_0/I)$. A plot of the absorbance versus the optical path-length is shown in Figure 1a. If the Beer-Lambert law is obeyed the plot is a straight line. The OH radicals were generated by pulse radiolysis of H_2O/SF_6 mixtures initiating the following reactions:





The OH radical decay was followed by monitoring the UV absorption signals at 309 nm at three different optical path lengths, 40, 80 and 120 cm. The optical band pass in the described experiments were 0.12 nm. The spectral resolution of the monochromator grating is 0.8 nm/mm.

An approximation to relate A to c is $A=(\epsilon cL)^n$ or $A^{1/n}=\epsilon cL$ [2]. In that equation n is an empirical constant that must be determined experimentally for the particular transient and experimental arrangement by examining the effect of c and L on A . The latter relation can be used to calculate c from the experimental absorbance. The exponent, n , can be determined from a plot of $\log A$ versus $\log L$, which is a straight line with the slope n . Such a plot is shown in Figure 1b. Figure 1c shows a plot of $A^{1/n}$ versus L . The straight line indicates that the modified Beer-Lambert law is obeyed.

This exponent, n , is further used to modify the transients before analysis of the kinetics. Figure 2a shows an OH-transient without correction and Figure 2b shows the same transient corrected with the n -factor 0.637. Instead of plotting the absorbance, A , versus time as in Figure 2a the absorbance raised to $1/n$ is plotted. The solid line through the experimental curve in Figure 2b was determined by detailed computer simulation of the experimental data taking the reactions (3) and (4a+b) into account. The following rate constants were used: $k_3=1.2 \times 10^{10}$ [3], $k_{4a}=9.0 \times 10^9 \text{ M}^{-1}\text{s}^{-1}$ [4] and $k_{4b}=1.0 \times 10^9 \text{ M}^{-1}\text{s}^{-1}$ [4]. The fit is good which indicates that this way of treating problems with non-Beer's law behaviour is correct. However, the uncertainty of the exponent, n , results in an additional uncertainty of at least $\pm 10\%$ of the corrected data.

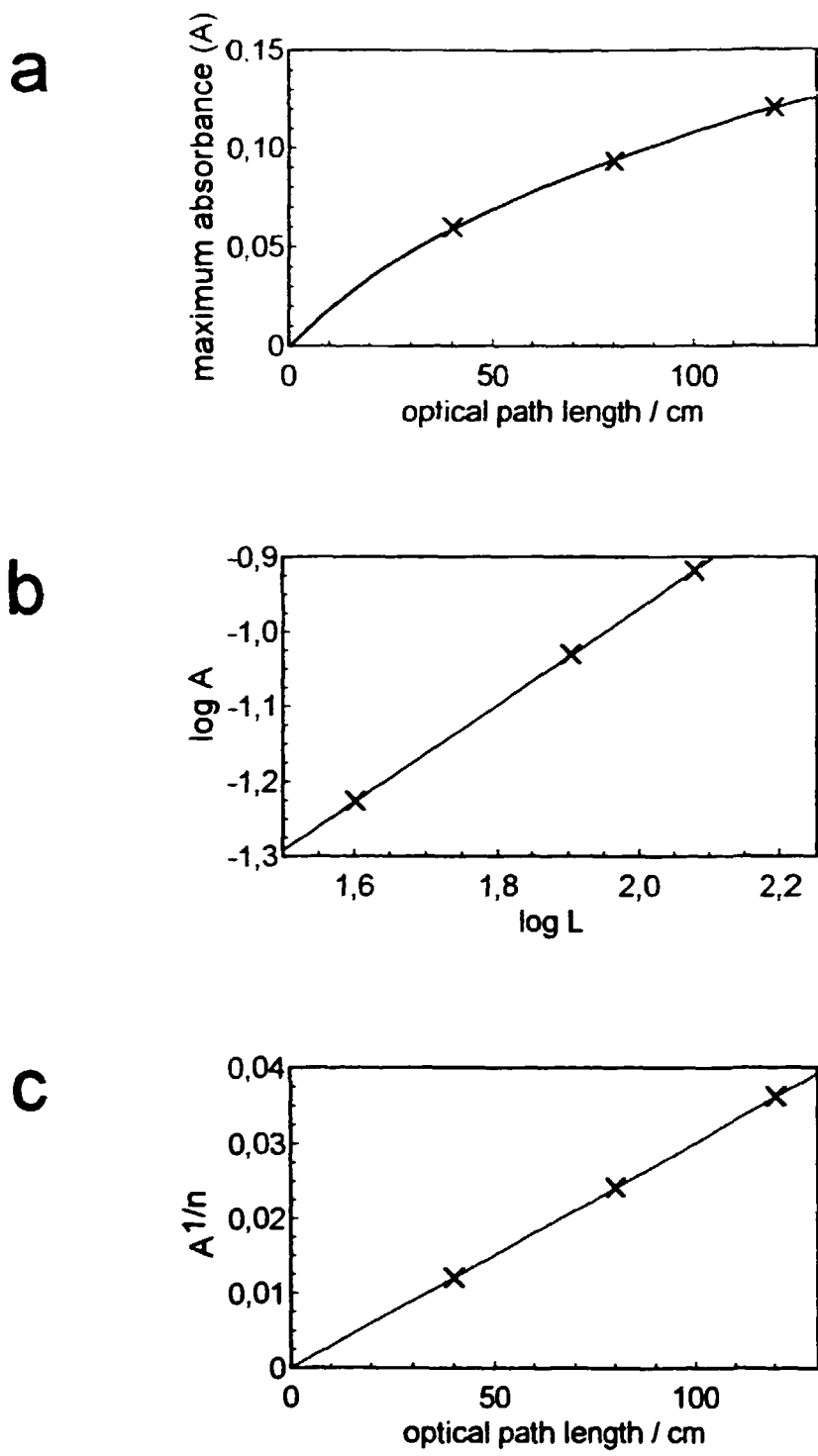


FIGURE 1. Measurements of the relation between optical path length, L , and OH radical absorbance monitored by the radical UV absorption at 309 nm by pulse radiolysis of 10 mbar H_2O and 990 mbar SF_6 . The optical band pass is 1.2 Å. The absorbance is calculated as $\log(I_0/I)$. The slope in Figure b is 0.637 which also is the n -factor.

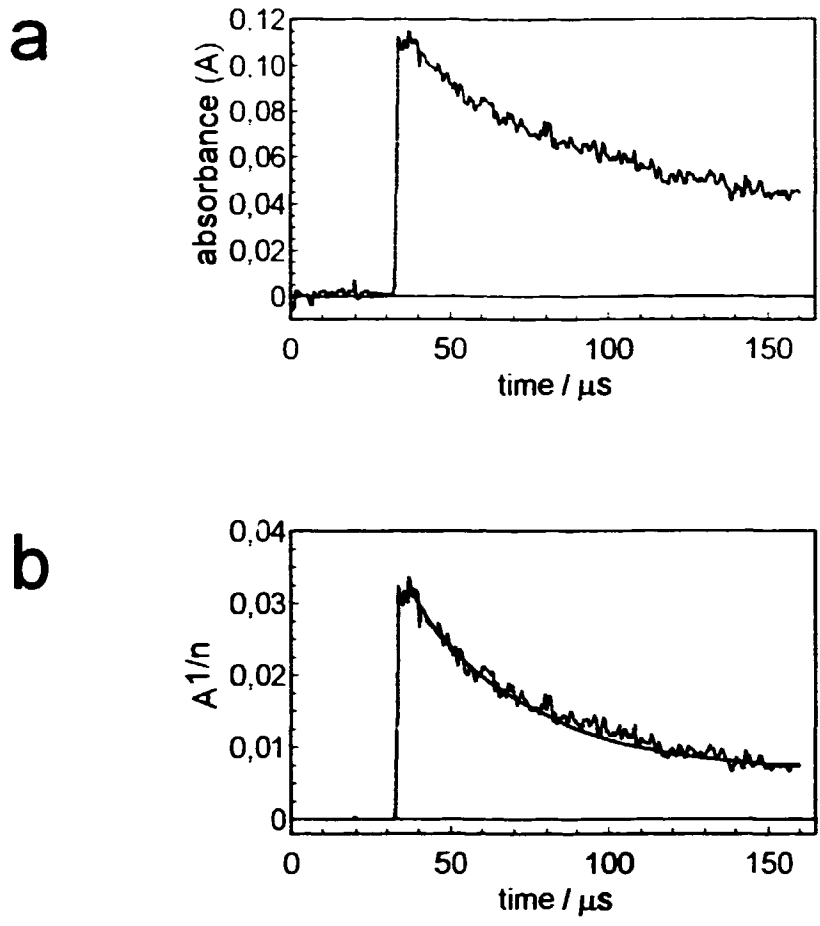


FIGURE 2. Figure a shows an OH transient without correction. The same corrected transient is shown in Figure b using an n-value of 0.637. The solid line is that predicted by modelling. The OH radicals were generated by pulse radiolysis of 10 mbar H₂O and 990 mbar SF₆ and monitored by the UV absorption at 309 nm. The optical band pass is 1.2 Å and the path length is 120 cm. The absorbance is calculated as $\log(I_0/I)$.

4.2 Wall reactions

One possible source of error in the interpretation of the experimental data is the loss of radicals by terminating wall reactions. For a gas containing only one type of molecules the mean molecular speed, u , is given by kinetic theory to be [5]:

$$u = (8kT/(\pi m))^{1/2}$$

where m is the molecular mass and k is the Boltzmann constant.

The following is a rough calculation of the additional error due to wall reactions for two of the most studied species, methyl radicals and fluorine atoms. In those calculations only the analyzed space in the reaction cell is taken into account, i. e. the volume covered by the electron beam. This volume is approximately 1 litre. The only walls within this space are the mirrors (see Figure 2 in Paper 1) with a total surface area of $4.6 \times 10^{-3} \text{ m}^2$.

For methyl radicals with a molar mass of 15 g the mean molecular speed is 648 m/s and for fluorine atoms with a molar mass of 19 g the molecular speed is 576 m/s at room temperature based on calculations using the above mentioned formula. The half-life for the pure methyl radical self-reaction is usually between 5 and 15 μs depending on the experimental conditions. The corresponding travelled distances during one half-life are 3.2 and 9.7 mm respectively. The volume from the mirrors and 9.7 mm out is $4.5 \times 10^{-5} \text{ m}^3$ which corresponds to 4.5% of the total volume. Shorter half-lives result of course in smaller portions. If the molecules were homogenously distributed in the reaction cell and if all the molecules included in this theoretical volume in front of the mirrors would move in the same direction towards the mirror surfaces the maximum error in the measured number of molecules generated would be 4.3%. A more likely case is that only about 1/6 of those molecules would move in the same direction. In this case the

error is only 0.8%. The half-life for fluorine atoms is only a few μs with a corresponding travelled distance of approximately 1 mm. The error in the measurement of the F-atom concentration is less than 0.1% based on similar calculations as for methyl radicals.

One source of error in the calculations above is that those assume that the molecules or atoms can travel towards the walls without hitting other molecules. The mean free path way, l , depends on the collision diameter, σ , and the number of molecules per unit volume, ρ , according to the following formula [6]:

$$l = (2^{1/2} \pi \sigma^2 \rho)^{-1}$$

In the experiments performed at Linköping mixtures of several gases are always used. This means that it is difficult to calculate a correct collision diameter. However, the mean free path way is much shorter than the above calculated travelled distances which means that in reality the probability of hitting another molecule is much higher than the probability of reaching the mirror surface. This reduces the calculated errors even more.

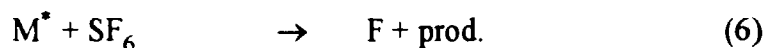
The conclusion of this discussion is that the wall-reactions are of no importance and well within the experimental error and thus these can be neglected in the evaluation of the experimental data.

4.3 The maximum radical concentration in different bath gases

A wide range of free radicals can be produced by the H-atom abstraction reaction of F-atoms with suitable hydrogen containing species:



The F-atoms were in our studies produced by pulse radiolysis of M/SF₆ mixtures. The initial F-atom concentration depends on the bath gas, M. The maximum F-atom concentration obtained in three different bath gases, SF₆, Ar and He, were tested by pulse radiolysis of M/SF₆/CH₄ mixtures, where M is the bath gas, initiating the following reactions:



By monitoring the maximum CH₃ concentration by the UV absorption at 216.4 nm a comparison of the different bath gases could be obtained. The maximum CH₃ concentration is assumed to be equal to the maximum F-atom concentration.

The gas compositions were 2 mbar CH₄ (which is above the saturation point), 50 mbar SF₆ and 948 mbar of the tested bath gas. Additional measurements of the maximum CH₃ concentration were made with only 2 mbar CH₄ and 50 mbar SF₆. This concentration was subtracted from the other measurements to obtain the concentration obtained only by the studied bath gas. In the case when M=SF₆ 948 mbar of SF₆ was mixed with 2 mbar of CH₄ and no subtraction was made. The result is given in Table 1.

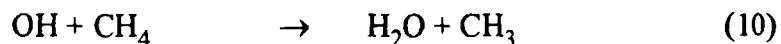
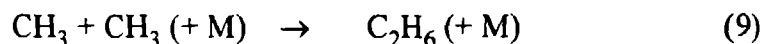
TABLE 1. Comparison of the efficiencies for different third bodies.

| Third body | [CH ₃] _{max} / μM |
|-----------------|--|
| SF ₆ | 1.41 |
| Ar | 0.34 |
| He | 0.06 |

Note: The subtracted CH₃ concentration is 0.09 μM.

4.4 Kinetics of the reaction between methyl and hydroxyl radicals

The kinetics of the reaction between methyl and hydroxyl radicals (8) using SF₆ as bath-gas is treated in Paper 2. Additional measurements of the rate constant for this reaction was made using Ar and He as bath-gases. The procedure for these additional measurements is the same as that described in Paper 2, and is therefore not described in detail in this section. The reaction (8) was initiated by pulse radiolysis of M/SF₆/CH₄/H₂O mixtures, resulting in the following reactions in addition to reactions (3), (4a+b), (5), (6) and (7):



The formation and decay of CH₃ radicals was followed at several [H₂O]/[CH₄] ratios by monitoring the transient UV absorption signals at 216.4 nm. The value of the rate constant for reaction (8) was obtained by detailed computer simulation of the experimental data. The experimental procedure and the procedure for data evaluation are described in Paper 2 as well as the rate constants used for modelling. The experimental conditions as well as the results of the computer modelling are listed in Table 2. As a comparison the results of the measurements performed in pure SF₆, reported in Paper 2, are included in the table.

Figures 3a-c and 4a-c show examples of the best fits of the model curves to the experimental curves for the measurements performed in Ar and He respectively using the rate constants listed in Paper 2 together with the k₈ values listed in Table 2. In the absence of water the methyl radical decay was second order for all the studied bath gases in accordance with the self-reaction (9).

TABLE 2. Conditions to monitor the CH₃-decay in the reaction system
M/SF₆/CH₄/H₂O (λ=216.4 nm, 4Å band pass, T=298 K).

| M | P(M) (mbar) | [F] ₀ (μM) | 10 ⁻¹⁰ k ₈ (M ⁻¹ s ⁻¹) | No. of experiments |
|-----------------|----------------|--------------------------|--|-----------------------|
| SF ₆ | 1000 | 0.40 ⁽¹⁾ | 7.8±0.7 | 50 |
| | 500 | 1.20 | 7.3±0.8 | 42 |
| | 170 | 0.41 | 6.0±0.3 | 36 |
| | 85 | 0.20 | 5.8±0.3 | 72 |
| Ar | 950 | 0.43 | 5.7±0.7 | 32 |
| | 450 | 0.25 | 4.5±0.5 | 26 |
| | 200 | 0.13 | 4.3±0.3 | 35 |
| He | 950 | 0.17 | 4.6±0.6 | 51 |
| | 450 | 0.14 | 4.3±0.7 | 55 |
| | 200 | 0.13 | 4.3±0.3 | 25 |

(1) reduced electron dose

Note: The SF₆ partial pressure was 50 mbar in all the experiments performed in Ar and He.

The k₈-value in 950 mbar argon and 50 mbar SF₆ was also monitored by Anastasi et. al. [3]. Their reported value, (5.7±0.8)×10¹⁰ M⁻¹s⁻¹ is in exact agreement with our value. This agreement must be taken as a good indication of the reliability of the reported results. We did not observe any pressure dependence of k₈ between 450 and 200 mbar He. One possible explanation to this is that the SF₆ in these mixtures dominates and that the additional effect of the He is within the experimental error limits. This might also be the case in 200 mbar Ar. The initial fluorine atom concentration obtained by pulse radiolysis of 50 mbar SF₆ and a few mbar CH₄ is 0.11 μM. This also shows that the additional He only has a minor effect.

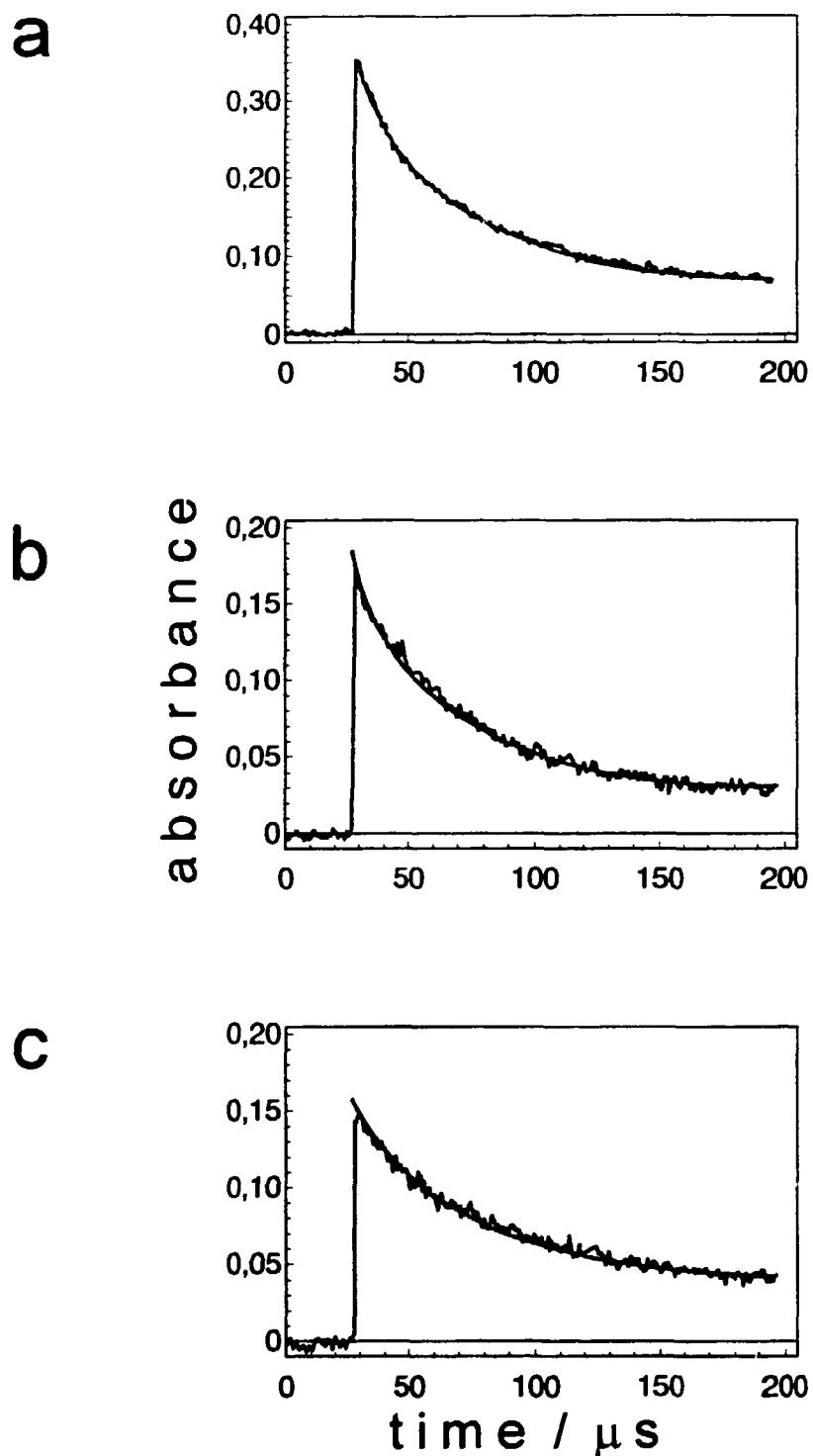


FIGURE 3. CH₃ radical decay monitored at 216.4 nm after single-pulse irradiation of Ar/SF₆/CH₄/H₂O mixtures. The solid lines are predicted by modelling. $A = \log(I_0/I)$. The optical band pass is 4 Å, $p(\text{SF}_6) = 50$ mbar and $L = 80$ cm. (a) $p(\text{Ar}) = 950$ mbar, $p(\text{CH}_4) = 3$ mbar and $p(\text{H}_2\text{O}) = 0$ mbar; self-reaction with $\tau = 35.1$ μs for $[\text{CH}_3]_{\text{max}} = 0.41$ μM; $k_g = 3.5 \times 10^{10}$ M⁻¹s⁻¹. (b) $p(\text{Ar}) = 950$ mbar, $p(\text{CH}_4) = 2.2$ mbar and $p(\text{H}_2\text{O}) = 6.6$ mbar; $\tau = 36.3$ μs for $[\text{CH}_3]_{\text{max}} = 0.22$ μM; $k_g = 5.7 \times 10^{10}$ M⁻¹s⁻¹. (c) $p(\text{Ar}) = 450$ mbar, $p(\text{CH}_4) = 3$ mbar and $p(\text{H}_2\text{O}) = 3$ mbar; $\tau = 63.5$ μs for $[\text{CH}_3]_{\text{max}} = 0.19$ μM; $k_g = 4.5 \times 10^{10}$ M⁻¹s⁻¹.

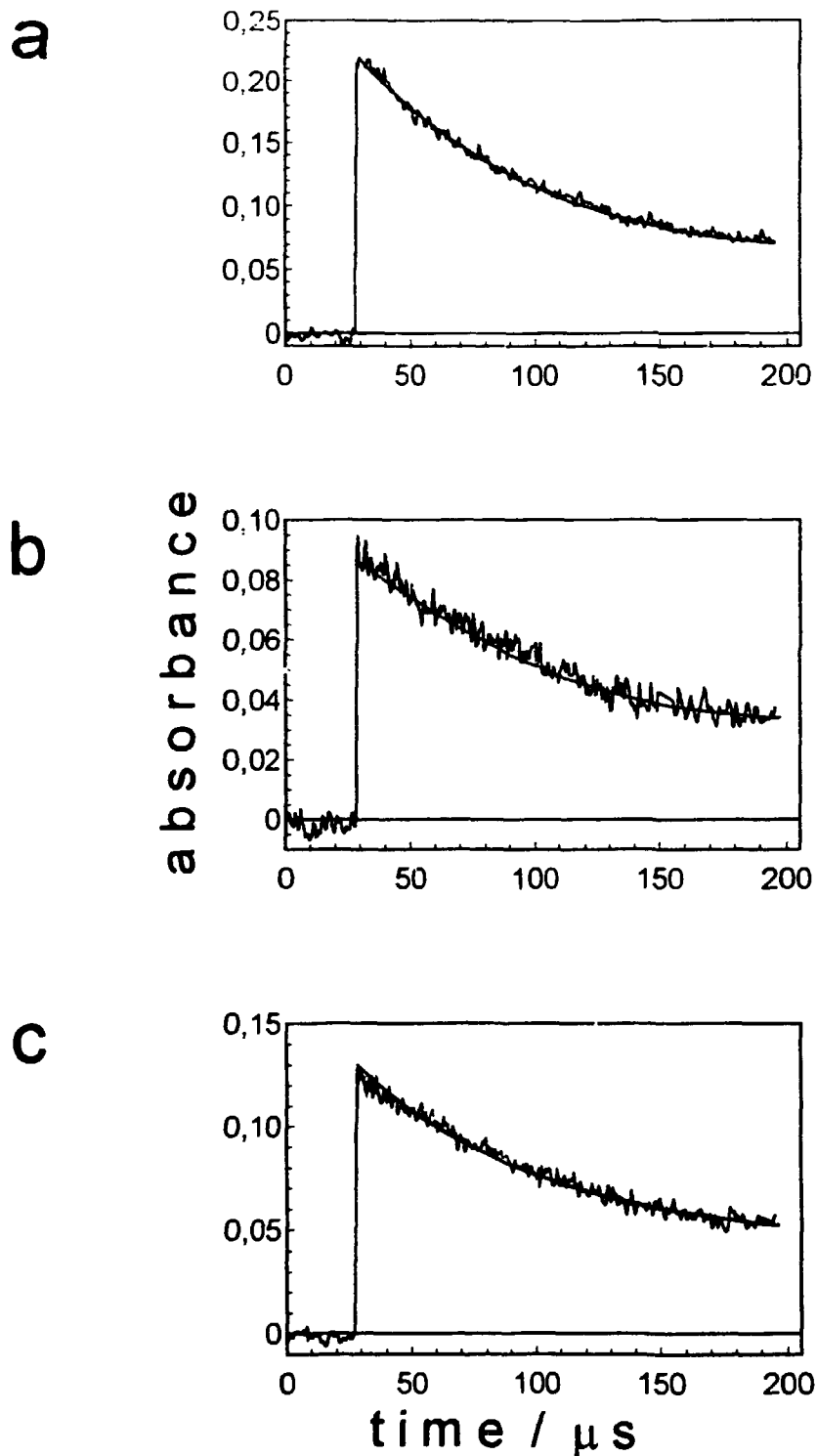


FIGURE 4. CH_3 radical decay monitored at 216.4 nm after single-pulse irradiation of $\text{He}/\text{SF}_6/\text{CH}_4/\text{H}_2\text{O}$ mixtures. The solid lines are predicted by modelling. $A = \log(I_0/I)$. The optical band pass is 4Å, $p(\text{SF}_6) = 50$ mbar and $L = 120$ cm. (a) $p(\text{He}) = 950$ mbar, $p(\text{CH}_4) = 5$ mbar and $p(\text{H}_2\text{O}) = 0$ mbar; self-reaction with $\tau = 86$ μs for $[\text{CH}_3]_{\text{max}} = 0.17$ μM ; $k_8 = 3.5 \times 10^{10}$ $\text{M}^{-1}\text{s}^{-1}$. (b) $p(\text{He}) = 950$ mbar, $p(\text{CH}_4) = 2.0$ mbar and $p(\text{H}_2\text{O}) = 10.0$ mbar; $\tau = 108.0$ μs for $[\text{CH}_3]_{\text{max}} = 0.07$ μM ; $k_8 = 4.6 \times 10^{10}$ $\text{M}^{-1}\text{s}^{-1}$. (c) $p(\text{He}) = 450$ mbar, $p(\text{CH}_4) = 3$ mbar and $p(\text{H}_2\text{O}) = 3$ mbar; $\tau = 114.0$ μs for $[\text{CH}_3]_{\text{max}} = 0.11$ μM ; $k_8 = 4.3 \times 10^{10}$ $\text{M}^{-1}\text{s}^{-1}$.

Acknowledgements

I wish to thank my supervisor Prof. Anders Lund for his encouragement and guidance and for all valuable discussions during this work. I have enjoyed our collaboration very much. Furthermore I would like to thank Prof. Hilbert Christensen for introducing me to pulse radiolysis.

I have special thanks to Dr. Gharib Mahmoud who during the last year has been working at our laboratory. We have had many fruitful, sometimes endless, discussions. He has also done a great job with the equipment which he improved in many ways.

Dr. Palle Pagsberg and Alfred Sillesen at Risø National Laboratory, Denmark, are acknowledged for their invaluable help during the construction of the equipment and for their support during the experimental period. I am also thankful for their patience with all my questions.

I would also like to thank Prof. Emil Ratajczak, the Medical Academy in Wrocław, Poland who spent three months at our laboratory. During his stay at Linköping he initiated several experimental studies and taught me a lot about gas-phase kinetics.

Finally, I would like to express my deep gratitude to my wife Cia for her patience and encouragement.

References

1. J. Nicholas, *Chemical Kinetics a Modern Survey of Gas Reactions*, (Harper & Row Ltd., London, 1976).
2. M. C. Sauer Jr., in: *Advances in Radiation Chemistry*, Vol. 5, eds. M. Burton and J. L. Magee (John Wiley & Sons, New York, 1976 p. 97).
3. C. Anastasi, S. Beverton, T. Ellermann and P. Pagsberg, *J. Chem. Soc. Faraday Trans.*, 87 (1991) 2325
4. NASA Chemical Kinetics and Photochemical Data, Evaluation No. 9, (JPL Publication, Pasadena, 1990, p. 90).
5. K. J. Laidler, *Chemical Kinetics* (Harper & Row, Publishers, Inc., 1987).
6. R. A. Alberty, F. Daniels, *Physical Chemistry* (John Wiley & Sons, New York, 1980).

Summary of papers

Paper 1

This paper describes in greater detail than in the introduction to this thesis the equipment used for the studies of radical reaction kinetics in the gas phase. In addition the effect on the kinetics of the electron dose inhomogeneity is calculated. The conclusion is that the error is less than 3% which means that the measured rate constant is not seriously affected by the inhomogeneity of the radiation dose.

Paper 2

This paper presents an experimental study of the kinetics of the cross-reaction between methyl and hydroxyl radicals as well as calculations of the high and low pressure limiting rate constants for this reaction. The reaction was initiated by pulse radiolysis of $\text{CH}_4/\text{H}_2\text{O}/\text{SF}_6$ mixtures at four total SF_6 pressures, 85, 170, 500 and 1000 mbar. The experiments were performed at room temperature. The radicals were produced by H-atom abstraction of CH_4 and H_2O by F-atoms. The CH_3 radical decay was followed by monitoring the UV absorption signals at 216.4 nm. The rate constant for the cross-reaction was determined by detailed computer simulation of the experimental data. A pressure dependence of the rate constant for the cross-reaction was clearly observed with values ranging from $(5.8 \pm 0.3) \times 10^{10} \text{ M}^{-1} \text{ s}^{-1}$ at 85 mbar to $(7.8 \pm 0.7) \times 10^{10} \text{ M}^{-1} \text{ s}^{-1}$ at 1000 mbar SF_6 . The high- and low-pressure limiting rate constants were calculated. $k_{1,\infty}$ can for the temperature range 200-400 K be expressed as $k_{1,\infty} = (8.7 \pm 0.9) \times 10^{10} \times (T/300)^{0.13} \text{ M}^{-1} \text{ s}^{-1}$. The low-pressure limiting rate constant can at room temperature be expressed as $k_{1,0}/[\text{SF}_6] = (2.6 \pm 2.3) \times 10^{15} \text{ M}^{-2} \text{ s}^{-1}$.

Paper 3

An experimental study of the reaction of ethyl radicals with hydroxyl radicals is described in this paper. In addition, the ethyl radical spectrum was monitored and is described as well. This spectrum shows two absorption bands centered at 205 and at 245 nm. The ϵ -value for the 205 nm band, which is the strongest, is $(2000 \pm 245) \text{ M}^{-1} \text{ cm}^{-1}$. The radicals were generated by pulse radiolysis of $\text{C}_2\text{H}_6/\text{H}_2\text{O}/\text{SF}_6$ mixtures and the C_2H_5 radical decay was followed by monitoring the UV absorption at 205 nm. In addition the formation of methyl and hydroxymethyl were monitored. These radicals are products formed in two possible reaction channels. The experiments were performed at room temperature and at three different total SF_6 pressures, 250, 500 and 1000 mbar. No pressure dependence of the rate constant for the investigated reaction was observed for the studied pressure range. The overall k -value, including the different reaction channels, that was obtained by computer simulation of the experimental data, is $(7.1 \pm 1.0) \times 10^{10} \text{ M}^{-1} \text{ s}^{-1}$. The high-pressure limiting rate constant for this reaction was calculated to be $(7.7 \pm 1.0) \times 10^{10} \text{ M}^{-1} \text{ s}^{-1}$ for the temperature range 200-400 K. The low-pressure limiting rate constant should at room temperature not be lower than $10^{17} \text{ M}^{-2} \text{ s}^{-1}$.